



THE UNIVERSITY *of* EDINBURGH

Edinburgh Research Explorer

Separation of large-scale structure and ripples on sand mounds

Citation for published version:

Borthwick, A, Taylor, P, Huang, J, Garcia-Hermosa, MI, Sun, J, Stansby, PK & Soulsby, RL 2012, 'Separation of large-scale structure and ripples on sand mounds' Proceedings of the ICE - Engineering and Computational Mechanics, vol 165, no. EM1, pp. 15-24., 10.1680/eacm.2012.165.1.15

Digital Object Identifier (DOI):

[10.1680/eacm.2012.165.1.15](https://doi.org/10.1680/eacm.2012.165.1.15)

Link:

[Link to publication record in Edinburgh Research Explorer](#)

Document Version:

Other version

Published In:

Proceedings of the ICE - Engineering and Computational Mechanics

General rights

Copyright for the publications made accessible via the Edinburgh Research Explorer is retained by the author(s) and / or other copyright owners and it is a condition of accessing these publications that users recognise and abide by the legal requirements associated with these rights.

Take down policy

The University of Edinburgh has made every reasonable effort to ensure that Edinburgh Research Explorer content complies with UK legislation. If you believe that the public display of this file breaches copyright please contact openaccess@ed.ac.uk providing details, and we will remove access to the work immediately and investigate your claim.



Editorial Manager(tm) for Engineering and Computational Mechanics
Manuscript Draft

Manuscript Number:

Title: Separation of large-scale structure and ripples on sand mounds

Article Type: Paper

Corresponding Author: Professor Paul Taylor, Ph.D

Corresponding Author's Institution: University of Oxford

First Author: Paul H Taylor, MA, PhD

Order of Authors: Paul H Taylor, MA, PhD; Alistair Borthwick; Peter Stansby; Isabel Garcia-Hermosa; Jingmin Huang; Richard Soulsby

Abstract: A simple method is proposed for the separation of large-scale structure from small-scale ripples during the evolution of an isolated sand hill or spoil heap eroded by an oscillatory or steady flow by bed-load transport. This method is based on Hermite functions, a mother Gaussian hill and derivatives modified to be orthogonal. It is straightforward to apply and could be used to characterise the geometric properties of any isolated localised hill-like feature such as pollution concentration levels away from an outfall.

Separation of large-scale structure and ripples on sand mounds

By P. H. Taylor¹, J. Huang², M. I. García-Hermosa³, P. K. Stansby⁴,

A. G. L. Borthwick¹ and R.L. Soulsby⁵

¹ Professor, Dept. of Engineering Science, Oxford University, Parks Road, Oxford OX1 3PJ, U.K.

² Career Development Fellow, Dept. of Engineering Science, Oxford University

³ PhD student, Dept. of Engineering Science, Oxford University and Research Assistant, School of Mechanical, Aerospace and Civil Engineering, Manchester University

⁴ Professor, School of Mechanical, Aerospace and Civil Engineering, Manchester University

⁵ Technical Director, HR Wallingford and Visiting Professor, Dept. of Engineering Science, Oxford University

Keywords: morphodynamics, ripples, bed forms, Hermite functions

ABSTRACT

A simple method is proposed for the separation of large-scale structure from small-scale ripples during the evolution of an isolated sand hill or spoil heap eroded by an oscillatory or steady flow by bed-load transport. This method is based on Hermite functions, a mother Gaussian hill and derivatives modified to be orthogonal. It is straightforward to apply and could be used to characterise the geometric properties of any isolated localised hill-like feature such as pollution concentration levels away from an outfall.

1. INTRODUCTION

The evolution of the sea-bed and the beds of rivers due to the motion of sediment is a complex problem coupling hydrodynamics with morphological changes. Even the description of the geometric structure resulting from flow over an isolated sand mound is difficult. This paper presents a method for separating large and small-scale geometric features on a sand mound exposed to steady and oscillatory flows. This separation is required to permit characterisation and modelling of the evolution of the bulk properties of a mound and also the development of the ubiquitous smaller-scale ripple features.

Whilst 2-D Fourier or wavelet filtering could achieve a reasonable extraction of the large-scale structure, we wanted a clean separation with a minimum of computational effort. A simple methodology was developed to analyse the experimental data for comparison with numerical predictions. The methodology is based on using the set of Hermite orthogonal functions (a

1
2
3
4 Gaussian mound and its derivatives, modified to be orthogonal) that fit the experimental data,
5 and help separate the bed mound from the smaller-scale laboratory features and noise. Examples
6 of the successful separation achieved for sand banks in large-scale experiments at the U.K.
7 Coastal Research Facility.
8
9

10
11 The proposed method is suitable for the characterisation of any isolated hill-like feature and
12 would aid the comparison of numerical simulations and physical experiments by treating each in
13 an identical manner.
14
15
16
17

18 2. CHOICE OF FUNCTIONS TO DESCRIBE LARGE-SCALE STRUCTURES

19 Amongst the requirements to fit the large-scale shape of an isolated mound are that a suitable
20 fitting function $g(x)$ (where x is distance in the horizontal) should have the following properties:
21
22

- 23 • $g(x)$ has its peak value when x is near to 0;
- 24 • $g(x) > 0$ so the basic shape is a single strongly localised hump
- 25 • $g(x) \rightarrow 0$ as $|x| \rightarrow \infty$
- 26 • The set of functions based on $g(x)$ and used for the fitting should be orthogonal.
- 27
- 28
- 29
- 30
- 31
- 32

33 Because of these requirements and for simplicity, a simple Gaussian profile was adopted as
34 $g(x)$. Initially we consider 1-D fits to the height of a hill along a horizontal slice in the x -
35 direction. The generalisation to a hill in 2-D is given later. The orthogonality requirement is
36 necessary so that there should be no ambiguity in the identification of components contained
37 within the mound. Since the aim is to fit arbitrarily shaped mounds as they evolve, a simple and
38 robust representation is required.
39
40

41 If the well behaved function $g(x)$ and all its derivatives decay smoothly to zero as $|x| \rightarrow \infty$, then
42
43

44
45 the integral $\int_{-\infty}^{\infty} \frac{dg}{dx} g(x) dx = \int_{-\infty}^{\infty} \frac{1}{2} \frac{d}{dx} (g(x))^2 dx = 0$ for any $g(x)$.
46
47
48

49 Similar results hold for the product of $g(x)$ multiplied by any other odd order derivatives and the
50 product of any even and odd derivatives, as can be shown simply by integration by parts.
51 However, the integrals of $g(x)$ and even derivatives, odd with other odd derivatives and even
52 with other even derivatives are not automatically zero unless the function has special properties.
53 Thus, we choose a convenient simple form for $g(x)$ and then insert small modifications to the
54 derivatives to enforce orthogonality.
55
56
57
58
59
60
61
62
63
64
65

1
2
3
4 For an arbitrary localised function, including a simple Gaussian, the integral
5
6 $\int_{-\infty}^{\infty} g(x) \frac{d^2 g}{dx^2} dx$, yields a non-zero quantity. Hence, the function and its 2nd derivative are
7
8
9 not orthogonal.

10
11 However, if the function $\frac{d^2 g}{dx^2}$ is replaced by a new function $d2g = \frac{d^2 g}{dx^2} - \varepsilon_{20} g$, then a
12
13
14
15 value for the parameter ε_{20} can be found such that orthogonality is imposed. We modify this
16
17 2nd derivative using the function $g(x)$ that we have already chosen. Thus, we actually subtract a
18
19 small Gaussian contribution from the original 2nd derivative. This small Gaussian contribution is
20
21 best associated with the leading order of $g(x)$ approximation to the shape of the mound (the
22
23 subscript 20 in ε_{20} denoting the modification of the 2nd derivative by the subtraction of a
24
25 Gaussian contribution, the 0th derivative).

26
27
28
29 In a similar manner for the 3rd derivative, there is automatic orthogonality with $g(x)$, but the
30
31 term has to be modified to enforce the orthogonality requirement with the slope of the Gaussian
32
33 hill. For the 4th derivative, orthogonality with both the original function $g(x)$ and also its now
34
35 modified 2nd derivative is enforced, via constants ε_{40} and ε_{42} .

36
37 Hence $d4g = \frac{d^4 g}{dx^4} - \varepsilon_{40} g - \varepsilon_{42} d2g$.

38
39
40
41 This pattern of modified orthogonal functions is simple to extend to arbitrary order with the aid
42
43 of MATHEMATICA™ to perform the manipulations.

44
45
46 A Gaussian function was used for $g(x)$ for two reasons. Firstly it is a well-studied smooth
47
48 function, and is versatile and ubiquitous in its applications and, secondly, it was chosen to be the
49
50 initial shape of the sand mound in much of our experimental work, García-Hermosa et al.^{1,2}.
51
52 With the choice of the Gaussian function, our derivation produces what are known in the
53
54 mathematical literature as Hermite functions for integer $n \geq 0$ (Kreyszig³ section 5.9,
55
56 Gradshteyn and Ryzhik⁴ section 8.95). There are easily accessed discussions of Hermite
57
58 functions at the websites: http://en.wikipedia.org/wiki/Hermite_polynomials,
59
60 <http://mathworld.wolfram.com/HermitePolynomial.html>. The identification of our modified derivatives
61
62 with Hermite functions provides mathematical legitimacy and rigour to our analysis technique.

1
2
3
4 However, our method of derivation is valid for any reasonable choice for $g(x)$ so long as it is
5 differentiable, not just for the Gaussian bell-shaped curve used here.
6
7

8
9
10 The Hermite functions are defined as $\psi_n(x) = \frac{1}{\sqrt{n! 2^n \sqrt{\pi}}} \exp[-x^2/2] H_n(x)$,

11
12 such that our previously derived modified Gaussian derivatives $dn_g = \psi_n(x)$. As required,
13 these functions are orthogonal on the entire x -axis:
14

$$15 \int_{-\infty}^{\infty} \psi_n(x) \psi_m(x) dx = \delta_{nm}, \text{ where } \delta_{nm} = 1 \text{ for } m = n, \text{ else } 0.$$

16
17
18 The Hermite polynomials within the functions are defined as
19

$$20 H_n(x) = (-1)^n \exp[+x^2] \frac{d^n}{dx^n} (\exp[-x^2]).$$

21
22 The first three terms are: $H_0(x) = 1$, $H_1(x) = 2x$, $H_2(x) = 4x^2 - 2$.
23
24

25 All the following terms can be obtained using the recurrence relation
26
27

$$28 H_{n+1}(x) = 2x H_n(x) - 2n H_{n-1}(x).$$

29
30 For the fitting procedure, we choose to use a Gaussian mound and its first 6 modified
31 derivatives, or equivalently the first 7 Hermite functions ($H_0 \rightarrow H_6$), to perform fits to the
32 physical experiments on evolving sand mounds. The basic Gaussian is taken as
33 $g(s, x) = e^{-s_x^2 x^2 / 2} (s_x^2 / \pi)^{1/4}$ where s_x is an inverse width parameter.
34
35
36
37
38
39
40
41
42

43 The shapes of the first 7 Hermite functions are shown in Figure 1, the Gaussian mother hill at
44 the top. As the order of the term is increased, each function captures finer scale structure whilst
45 remaining relatively well restricted to the region covered by the mother Gaussian hill. Also clear
46 in the figure is the alternating symmetric, skew-symmetric pattern of the terms. Note that all
47 Hermite functions other than the mother Gaussian hill are shown in positive and negative forms
48 to emphasise that their amplitudes may be of either sign, each higher order term representing a
49 particular perturbation away from the positive hill form for the mother Gaussian. Clearly a
50 simple summation of a set of functions of this type should be able to represent quite
51 complicated mound profiles in 1-D and also surface shapes in 2-D via products of Hermite
52 functions in the two horizontal coordinates.
53
54
55
56
57
58
59
60
61
62
63
64
65

1
2
3
4
5
6
7
8
9
10
11
12
13
14
15
16
17
18
19
20
21
22
23
24
25
26
27
28
29
30
31
32
33
34
35
36
37
38
39
40
41
42
43
44
45
46
47
48
49
50
51
52
53
54
55
56
57
58
59
60
61
62
63
64
65

FIGURE 1

The choice of how far along a Hermite series expansion to go is, of course, specific to each application. The same problem of truncation occurs for Fourier or wavelet decomposition. For our application to the U.K.C.R.F. sand mound data, the overall mound is initially ~ 4 m across, with ripples developing with a characteristic wavelength scale of ~ 0.7 m. Hence, we choose to go up to the 6th derivative (7th Hermite function) for terms to describe the overall hill shape. Some justification for this choice is provided later.

3. FITTING METHOD

The functional form outlined in the previous section is simple to generalise to allow the fitting of a hill described as a height in two horizontal co-ordinates, here $h(x, y)$. We choose to model the hill form as products of Hermite functions of the mean flow (x -) direction and the (y -) direction orthogonal to this. Whilst, in principle any Cartesian co-ordinate system could be used, we choose to use one orientated to match the geometric layout of the physical experiments.

The fitting procedure starts by finding the centre of gravity of the mound in the horizontal plane. This point becomes the origin of the co-ordinate system and the centre of the Gaussian mother hump. Then the height of the mound above the reference plane is written as:

$$h(x, y) \approx \sum_{i=0}^6 \sum_{j=0}^6 A_{ij} \psi_i(s_x, x) \psi_j(s_y, y) ,$$

where $h(x, y)$ is the measured shape of the mound, $\psi_i(s_x, x)$, $\psi_j(s_y, y)$ are Hermite functions of order i and j in the x - and y -directions, and s_x and s_y correspond to measures of the inverse widths of the mound in these same directions. Note again that we take the x -direction parallel to the mean flow, and y is the transverse direction.

The first stage of the fitting process is to estimate the global mound parameters s_x and through a simple least squares shape fit of the single mother Gaussian mound to the actual mound. There are then 49 A_{ij} coefficients to be determined by simple numerical integration

$$A_{ij} = \iint \psi_i(s_x, x) \psi_j(s_y, y) h(x, y) \, dx dy .$$

1
2
3
4 The first term and its coefficient A_{00} capture global information about the mound, as well as
5
6 almost all the volume. The second term A_{10} describes the leading order contribution to front-
7
8 back asymmetry along the flow direction and is particularly important in steady flow. The terms
9
10 with j odd describe asymmetric features across the mound perpendicular to the mean flow
11
12 direction.
13

14 4. EXPERIMENTAL SET-UP FOR THE STUDY OF SAND MOUND EVOLUTION

15
16 Figure 2 shows the experimental set-up. The mound of sand was located at the centre of a wide
17
18 flow channel constructed in the U.K. Coastal Research Facility at HR Wallingford. The working
19
20 section of the channel was 8 m across and had a smooth horizontal concrete floor. An array of
21
22 pumps was used to drive either a sinusoidal oscillatory or a steady flow through the working
23
24 section with a peak velocity of 0.5 m/s. Most experiments were performed for an isolated
25
26 mound on a bare concrete base although a few cases of the mound surrounded by a uniform
27
28 depth sand layer on the concrete were also performed. Further details are given in García-
29
30 Hermosa et al. ^{1,2,5}
31

32 FIGURE 2

33
34
35 In this paper we present detailed results for the oscillatory flow case of an initially fully
36
37 submerged sand mound on the bare concrete and then some results for comparison for the same
38
39 initial shaped mound in a steady flow. The first experiment is akin to the erosion and dispersal
40
41 of a sand hill or spoil heap dumped offshore in a tidal stream on a non-erodible bed, the second
42
43 to a sand hill in a wide river. In both cases the undisturbed water depth was 20 cm. The initial
44
45 shape of the mound was Gaussian and its height 15 cm.
46

47
48 In the first experiment the oscillation period of the bulk flow was 20 min and the experiment
49
50 was ended after 61 cycles when the bulk features of the bank had been almost completely
51
52 washed away. Periodically the flow was stopped and the water level gradually lowered,
53
54 allowing contours of the sand mound to be recorded at different times using a high-resolution
55
56 digital camera mounted directly above the centre of the mound. The water level was then raised
57
58 to the original level and the flow re-started. The contours were then manually digitised, a slow
59
60 and laborious process but one which gave much more accurate results than automatic
61
62
63
64
65

1
2
3
4 digitisation. These contours are then analysed to separate out the large-scale mound features
5 from the small-scale ripples using the methodology presented in this paper.
6
7

8 9 5. SEPARATION OF LARGE-SCALE FEATURES FROM SMALL-SCALE RIPPLES

10 Figure 3 shows a succession of views of the physical bathymetry for the oscillatory flow after 0,
11 1, 6, 12 and 61 cycles. The initial profile is a simple Gaussian shape, albeit truncated at a
12 distance of a radius of 2.5 m from the peak where the depth of sand on the concrete bed was 2
13 mm. The views on the left hand side are projections re-created using the PC graphics package
14 SURFER™ of the complete hill shape based on the raw contours, the middle views are of the
15 bulk mound shape extracted by Hermite fitting, the right-hand side views are of the small-scale
16 remainder, which we infer to be ripple structure. Each horizontal line of 3 projections has the
17 same vertical scale.
18
19
20
21
22
23
24

25
26 The separation of the large-scale and small-scale features is clear and unambiguous. It is self-
27 evident that the extraction method is working well. The only artefact visible is in the small-scale
28 structure after 0 and 1 cycles, a ring is visible in the ripple plot around the hump. This is related
29 to the spacing of the contours at vertical intervals of 1 cm above the concrete bed. Thus, the thin
30 sand layer beyond this out to the physical cut-off of the original Gaussian shaped mound at a
31 distance of 2.5 m from the mound centre is missed in the digitisation. At the physical cut-off,
32 the depth of the sand layer is ~2 mm. At later times this artificial feature associated with an
33 apparent step from 1 cm to the ground plane is washed out as sand is transported out and laid
34 down onto the bare concrete bed. Also visible initially are the very small 8-way irregularities
35 arising because the hill was constructed as a combination of 8 45° ‘cake-slices’ using wooden
36 templates.
37
38
39
40
41
42
43
44

45
46 As the experiment progresses and the hill evolves, it loses the initial simple Gaussian form. At
47 61 cycles, the centre of the remaining mound has moved ~2 m from its original location,
48 denoting either a very slight asymmetry in the forwards and backwards flow velocities or, less
49 likely, resulting from the direction of flow in the first half-cycle as a long-term memory effect.
50
51
52
53
54

55 FIGURE 3

56
57
58
59 Further details of the separation of large- and small-scale features are shown in Figure 4 as
60 vertical sections along the centre-line of the mound. The dashed horizontal lines denote the
61
62
63
64
65

1
2
3
4 heights used for the contour plots in Figure 6. This Figure shows both the measured data and
5 also the Hermite fits to the large-scale mound structure only. Clearly, the fits do a satisfactory
6 job at scale separation for the vertical sectional plots even at later times when the ripples are as
7 large as the underlying sand hump. The only artefact of the fit is a slight undershoot outside the
8 sand humps where the fits go slightly negative. This can be associated with a Gibbs-like
9 behaviour, familiar from Fourier theory when smooth fitting functions are used to model a slope
10 near-discontinuity. Here this occurs because the concrete bed is non-erodible. Within the mound
11 itself, the ripples are clearly visible. It is interesting to note that the largest ripple height at ~ 7
12 cm occurs early on in the evolution of the sand mound and persists for long times as the large-
13 scale features are washed away. Even after 61 cycles when the ripple half-height is similar to
14 the height of the overall hill and some of the deepest ripple troughs expose bare concrete, this
15 large ripple height is only reduced to 5 cm. Huang et al.⁶ presents more detailed analysis on the
16 ripple structure.

27
28 FIGURE 4

30
31 The question of how many terms that should be included in the Hermite function fit is
32 considered in Figure 5. This shows fits at various levels of approximation: from a single mother
33 Gaussian hump (the 0th order with just 1 coefficient), to 2nd (3 \times 3 coefficients), 4th (5 \times 5), 6th
34 (7 \times 7) and 10th order Hermite terms (11 \times 11). In our view the mound shown here, after 12
35 cycles in the form of vertical sections through the centre along the flow direction, is reasonably
36 well captured by the 6th order (7 \times 7) Hermite fits. The highest order fit is including some of the
37 ripple structure.

44
45 FIGURE 5

48 Table 1 shows the relative magnitudes of $|A_{ij}|$ for 10th order (11 \times 11) Hermite fits to the sand
49 mound after 12 and 61 cycles. Obviously the A_{00} contribution from the mother Gaussian is
50 dominant in each but at both times there are significant contributions to the overall shape from
51 higher order terms. These tail off beyond \sim the 6th order terms. At both times, a cut-off criterion
52 in the range 5-10 applied to the $|A_{ij}|$ coefficients justifies the choice of the 6th order fit. However,
53 we note that the coefficients beyond this are small but non-zero. Sufficiently high-order Hermite
54
55
56
57
58
59
60
61
62
63
64
65

function fits will start to resolve the ripple structure. As with all 2-D fitting methods, there is a question as to how to treat all coefficients further than a distance of N steps from the mother Gaussian (e.g. the A_{ij} terms with $i + j > N$, N being the fit order) once the order of the fit is chosen. Here we simply weight these terms $\propto 1$ for $\sqrt{i^2 + j^2} = N$, linearly down to $\propto 0$ for the diagonal term ($i = N, j = N$) furthest from the Gaussian mother hill. This is analogous to the smoothing commonly applied to the results of digital filtering in FFTs to mitigate anisotropy and ringing-type effects when transformed back into the physical domain.

TABLE 1

FIGURE 6

Figure 6 shows contour plots at three stages during the experiments. Being horizontal slices through the sand mound at 1 cm and 3 cm above the concrete bed, these show the geometric complexity of the ripples superimposed on top of the large-scale mound. The Hermite function Gaussian-based fits do a satisfactory job at smoothing these out without the loss of bulk information even for the highest contour at 3cm after 61 cycles, when the top of inferred large-scale mound is only just higher than this level. Although the original mound and the bulk oscillatory flow are symmetric, or as close to symmetric as experimentally possible, symmetry across the mound is completely lost for the ripples and degraded even for the large-scale structure. Further detailed analysis of the geometric changes for a wider range of experimental cases will be reported elsewhere.

We now turn to the steady flow case with an erodible sand hill on a concrete bed. Figure 7 shows the temporal evolution of the hill. Clearly there is a net migration of the hill downstream with time. Also the large-scale hill appears to be evolving towards the well-known crescent or barchan shape. This is particularly clear after 1 and 2 hours of flow. Now the second Hermite coefficient A_{10} , describing the leading order contribution to front-back asymmetry along the flow direction, is particularly important. As for the oscillatory flow case, we achieve a clear separation of local small-scale ripples from the overall shape.

1
2
3
4 At later times in the steady flow, the downstream slip-face of the hill approaches and passes
5 outside the observation window used for the digitisation. This leads to the artefact of a linear
6 vertical discontinuity at the edge of the window apparent after 3 hours. However, within the
7 main body of the visible portion of the mound we still achieve satisfactory scale separation.
8
9

10
11
12 FIGURE 7
13

14 15 16 6. CONCLUSION

17 An efficient and robust method has been proposed for the separation of large-scale and small-
18 scale features on an evolving sand mound in both oscillatory and steady flows. The large-scale
19 features are described using a Gaussian shape and associated orthogonal Hermite functions.
20 This works well both at fits over the horizontal plane to the whole hill and also when either
21 vertical or horizontal sections (height contours) are considered. The analysis makes use of large-
22 scale datasets obtained in the U.K. Coastal Research Facility at HR Wallingford.
23
24
25
26
27
28

29 The analysis method used here to extract large-scale features from the highly complex forms
30 seen in experiments on an evolving hill is also directly applicable to the results of numerical
31 simulations such as Apsley and Stansby⁷, Stansby et al.⁸, Huang et al.⁹ where the small-scale
32 ripple features are not usually resolved. Experimental comparison to and validation of numerical
33 simulations could be greatly improved if all the results were processed in the same way using
34 the Hermite functions.
35
36
37
38
39
40

41 We also consider that this approach could be helpful to model other problems in civil
42 engineering such as involving spreading away from a point where a separation of large-scale
43 and small-scale structure might yield useful information – an example could be pollutant
44 concentration variations away from an outfall in a tidal flow.
45
46
47
48
49

50 ACKNOWLEDGEMENT

51 The laboratory tests were supported by EPSRC grants GR/S73396 and GR/S73042 titled
52 ‘Shallow-water morphodynamics: a fundamental experimental and numerical study of
53 sandbanks’, held at the Universities of Manchester and Oxford.
54
55
56
57
58
59
60
61
62
63
64
65

1
2
3
4 REFERENCES

5 [1] García-Hermosa, M.I., Huang, J., Zhou, J.G., Stansby, P.K., Taylor, P.H., Soulsby, R.L., and
6 Borthwick, A.G.L. (2006) A fundamental experimental and numerical study of large scale
7 morphodynamics of sandbanks in steady and oscillatory flows. *Proc. ASCE 30th International*
8 *Conference on Coastal Engineering*, San Diego, 2006, pp 2701-2713.

9
10
11 [2] García-Hermosa, M.I., Huang, J., Stansby, P.K., Soulsby, R.L., Borthwick, A.G.L. and
12 Taylor, P.H. (2008) Interpretation of large-scale morphodynamic laboratory experiments: spoil
13 heaps and sandbanks. Abstract submitted to *ASCE 31st International Conference on Coastal*
14 *Engineering*, Hamburg, 2008.

15
16
17 [3] Kreyszig, E. (1993) *Advanced Engineering Mathematics*, 7th edition. John Wiley and Sons.

18
19
20 [4] Gradsteyn, I.S. and Ryzhik, I.M. (1965) *Table of Integrals, Series and Products*. 4th edition.
21 Academic Press.

22
23 [5] García-Hermosa, M.I., Huang, J., Borthwick, A.G.L., Zhou, J.G., Taylor, P.H., Soulsby,
24 R.L., and Stansby, P.K. (2007) Experimental observations and numerical modelling of the
25 evolution of sand mounds in steady and tidal flow. In preparation for submission to *Coastal*
26 *Engineering*.

27
28
29 [6] Huang, J., García-Hermosa, M.I., Stansby, P.K., Taylor, P.H., Soulsby, R.L., and Borthwick,
30 A.G.L. (2007) Ripple formation on sand mounds at large laboratory scale. Submitted to *ASCE J.*
31 *of Hydraulic Engineering*.

32
33
34 [7] Apsley, D.D. and Stansby, P.K. (2007) “Bed load transport with large slopes: a general
35 formulation within a general RANS flow solver”, under review with ASCE *Journal Hydraulic*
36 *Engineering*.

37
38 [8] Stansby, P.K., Huang, J., Apsley, D.D., García-Hermosa, M.I., Borthwick, A.G.L., Taylor,
39 P.H., and Soulsby, R.L. (2007) “Modelling sand mound dynamics in steady and oscillatory
40 flows”, in preparation.

41
42
43 [9] Huang, J., Borthwick, A.G.L., and Soulsby, R.L. (2007) 1-D modelling of fluvial bed
44 morphodynamics. *J. of Hydraulic Research*. (At printers)

1
2
3
4
5
6
7
8
9
10
11
12
13
14
15
16
17
18
19
20
21
22
23
24
25
26
27
28
29
30
31
32
33
34
35
36
37
38
39
40
41
42
43
44
45
46
47
48
49
50
51
52
53
54
55
56
57
58
59
60
61
62
63
64
65

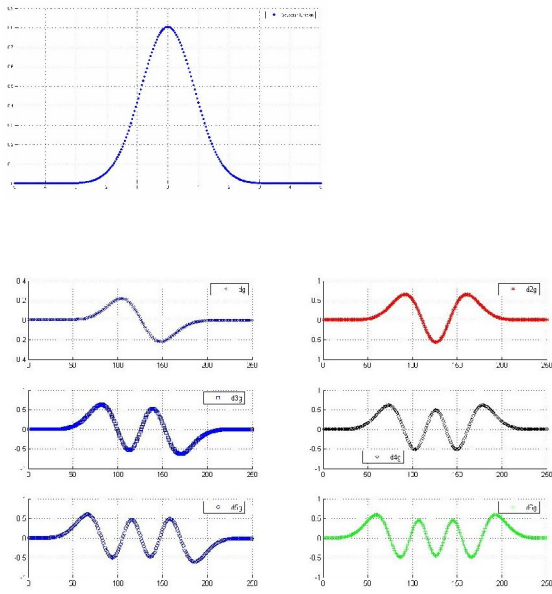


FIGURE 1. The first 7 Hermite functions, with the mother Gaussian hill at the top.

1
2
3
4
5
6
7
8
9
10
11
12
13
14
15
16
17
18
19
20
21
22
23
24
25
26
27
28
29
30
31
32
33
34
35
36
37
38
39
40
41
42
43
44
45
46
47
48
49
50
51
52
53
54
55
56
57
58
59
60
61
62
63
64
65

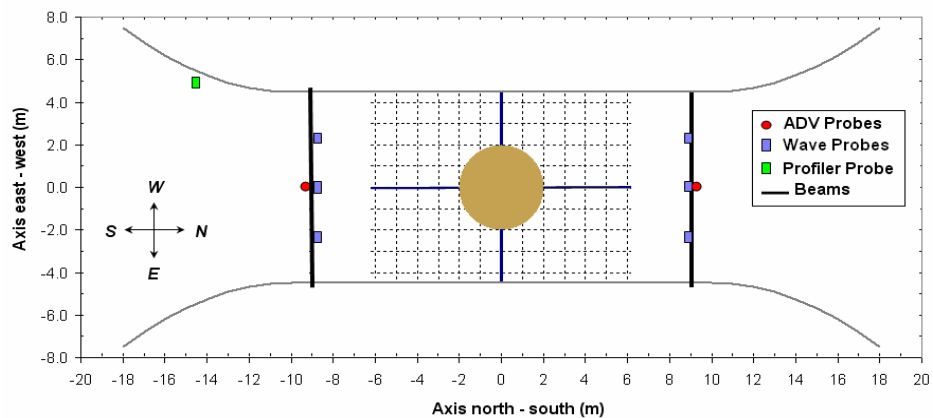


FIGURE 2. Experimental layout of the sand hill in the U.K.Coastal Research Facility.

1
2
3
4
5
6
7
8
9
10
11
12
13
14
15
16
17
18
19
20
21
22
23
24
25
26
27
28
29
30
31
32
33
34
35
36
37
38
39
40
41
42
43
44
45
46
47
48
49
50
51
52
53
54
55
56
57
58
59
60
61
62
63
64
65

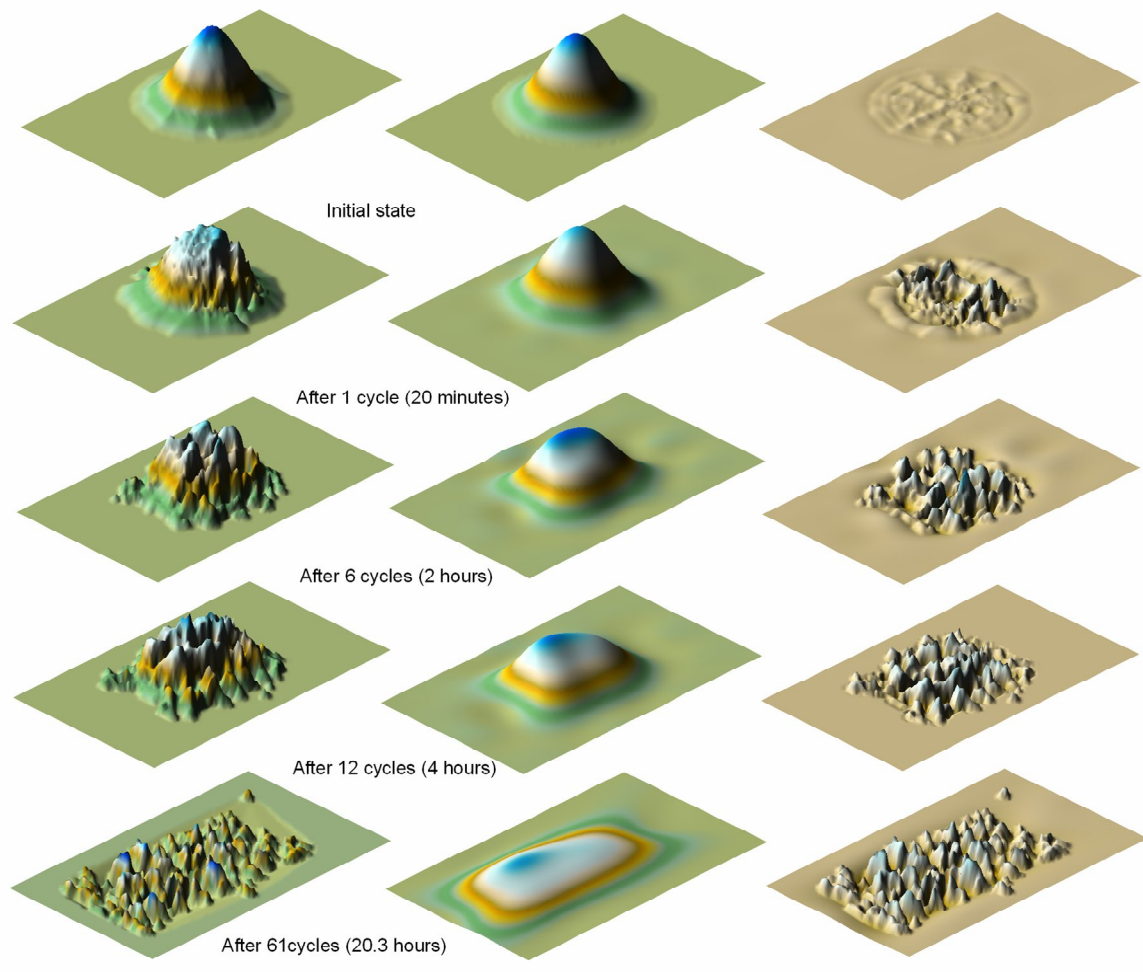


FIGURE 3.
Example of physical bathymetry (left), its 7×7 Hermite fit (centre) and inferred ripple structure (right), shown as isometric projections for the oscillatory flow case.

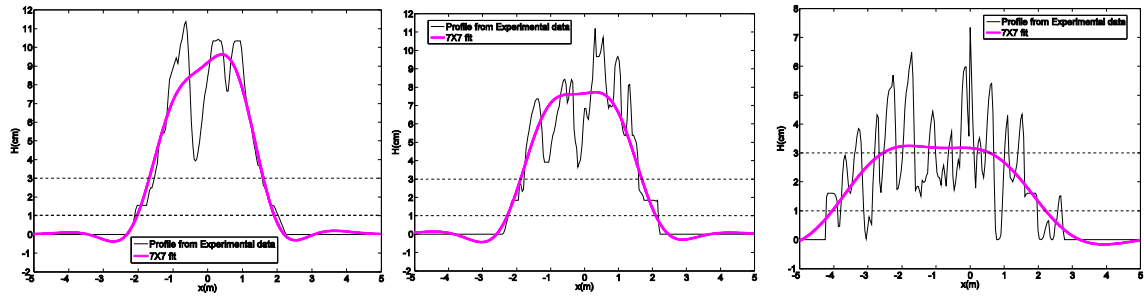


FIGURE 4
 Examples of scale separation using Hermite functions for an initially submerged Gaussian hill - vertical profiles along the mean flow x - direction with $y=0$ after 5, 12 and 61 cycles of oscillatory flow.

10	4	3	4	4	2	3	2	2	2	1	3
9	1	5	3	4	5	2	5	1	3	0	2
8	1	3	3	4	2	3	2	2	2	1	2
7	2	4	3	3	4	3	3	2	2	1	2
6	5	3	2	3	1	2	1	2	1	1	1
5	6	0	4	1	2	2	2	2	2	1	1
4	11	5	1	2	0	1	1	1	2	1	1
3	9	4	6	2	2	0	1	1	1	1	1
2	0	4	3	2	2	1	3	1	3	2	1
1	7	5	7	4	4	4	2	2	1	1	1
0	168	1	0	2	19	3	12	3	3	2	3
	0	1	2	3	4	5	6	7	8	9	10

10	0	1	0	1	0	1	0	0	0	0	0
9	1	2	0	0	0	2	0	3	0	3	0
8	1	2	1	1	0	1	0	1	0	1	0
7	1	1	0	0	0	1	0	2	0	2	0
6	6	2	1	2	0	2	0	1	0	1	1
5	1	0	0	0	0	0	0	1	0	1	0
4	11	2	1	2	1	1	1	0	2	0	2
3	2	0	2	1	1	2	0	1	0	0	1
2	0	2	3	1	2	1	4	2	4	1	4
1	3	5	6	4	2	4	2	4	3	3	2
0	99	3	0	4	12	1	8	1	3	2	2
	0	1	2	3	4	5	6	7	8	9	10

TABLE 1. Variation of amplitude coefficient $|A_{ij}|$ with order of the Hermite functions for 2-D fits after 12 and 61 cycles of oscillatory flow.

1
2
3
4
5
6
7
8
9
10
11
12
13
14
15
16
17
18
19
20
21
22
23
24
25
26
27
28
29
30
31
32
33
34
35
36
37
38
39
40
41
42
43
44
45
46
47
48
49
50
51
52
53
54
55
56
57
58
59
60
61
62
63
64
65

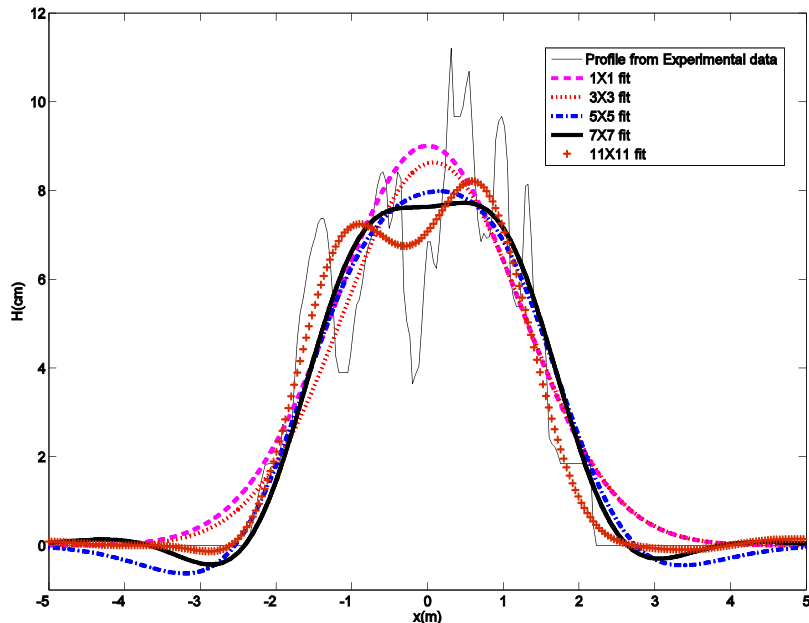


FIGURE 5. Examples of the effect of the order of the Hermite functions retained to describe the large-scale structure. Vertical profile of the hill along the mean flow x - direction with $y=0$ after 12 cycles of oscillatory flow, fits from (1×1) up to (11×11) .

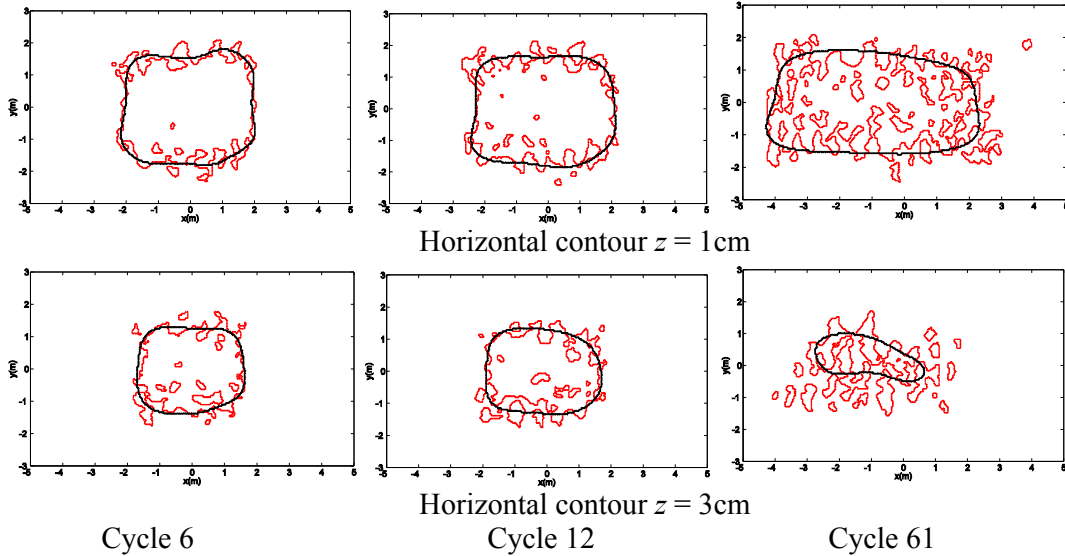


FIGURE 6. Examples of scale separation using Hermite functions for horizontal contours (z -fixed) of the measured hill and extracted large-scale structure in oscillatory flow.

1
2
3
4
5
6
7
8
9
10
11
12
13
14
15
16
17
18
19
20
21
22
23
24
25
26
27
28
29
30
31
32
33
34
35
36
37
38
39
40
41
42
43
44
45
46
47
48
49
50
51
52
53
54
55
56
57
58
59
60
61
62
63
64
65

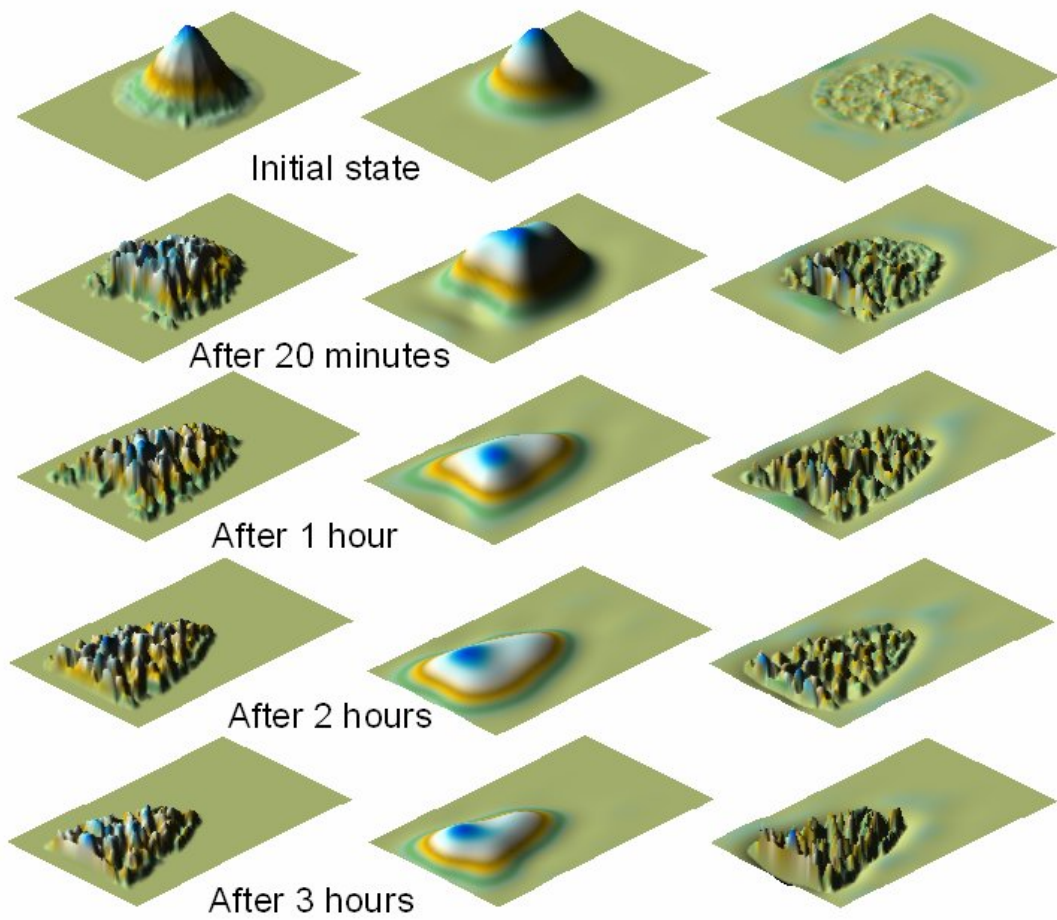


FIGURE 7
Examples of scale separation using Hermite functions for an initially submerged Gaussian hill in a steady flow.